Maximizing MR Signal for 2D UTE Slice Selection in the Presence of Rapid T2 Relaxation

M. Carl[1], J-T. Chiang[2], and M. Bydder[2]
[1]Global Applied Science Laboratory, GE Healthcare, San Diego, CA, United States, [2]University of California, San Diego, United States

Introduction: When imaging short or ultra short T_2 species, such as ligaments, tendons or cortical bone, the intrinsic T_2 can be on the same order as the RF duration τ, and the signal decay during the RF pulse may not be ignored [1]. In recent work [2,3] a generalized Ernst angle was developed for hard pulse excitation to maximize the available MR signal for 3D UTE imaging. Here we extend the analysis to slice selective shaped pulses used in 2D UTE. For 2D UTE, Robson et al [4] have shown significant effects of T2 decay during shaped RF pulses on signal amplitude and slice profile.

Theory: The two parameters that determine the flip angle for a shaped RF pulse are the time dependent magnetic RF field strength $B_1(t)$ and pulse duration τ. Solving the Bloch equations in the small tip angle approximation for the transverse and longitudinal magnetization for a single RF pulse, using a slice selection gradient $G(t)$ in the presence of T_2 relaxation leads to:

$$M_T(\tau,z) = \gamma M_0 e^{-\frac{\tau}{T_2}} e^{-i\gamma z\int_0^\tau G(t)dt} \int_0^\tau B_1(t) e^{\frac{t}{T_2}} e^{i\gamma z\int_0^t G(s)ds} dt \qquad [1a]$$

$$M_z(\tau,z) = M_0 - \gamma\int_0^\tau B_1(t) M_T(\tau,z) dt \qquad [1b]$$

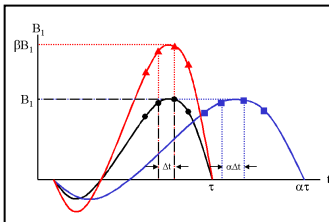

Fig.1: RF profile. Original profile (black), time-stretched (blue), and amplitude-stretched (red).

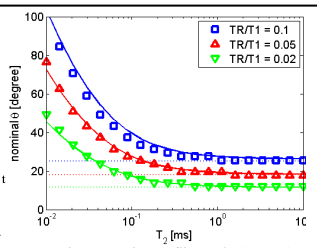

Fig.2a: Optimum flip angle (const τ)

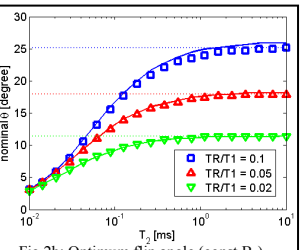

Fig.2b: Optimum flip angle (const B_1)

To a good approximation one can evaluate Eq.[1] at the center of the slice (z = 0), to simplifies the analysis. Solving Eq.[1] at z = 0 requires knowledge of $B_1(t)$, which with UTE sequences are VERSE corrected [5] and hence not in simple closed form. Therefore, it is more straightforward to integrate Eq.[1] numerically as discrete sums using the actual discrete waveforms profile of $B_1(n)$ (see Fig.1). We will assume that the RF pulse profile contains N points, has a raster time Δt corresponding to a duration of $\tau = N\Delta t$, and amplitude B_1. One can express the general RF duration τ and raster time Δt via a stretch factor α: ($\tau \rightarrow \alpha\tau$, $\Delta t \rightarrow \alpha\Delta t$) and the general RF amplitude by an amplitude scaling factor β: $B_1 \rightarrow \beta B_1$. This allows one to investigate the best duration of the pulse (best stretch factor α), and/or the best amplitude scaling (amplitude scaling factor β) to maximize the MR signal.

The steady state transverse magnetization can be calculated using the SPGR condition:

$$M_{SS}(\alpha\tau,\beta B_1) = \frac{(1-E_1)}{1-E_1\frac{M_z}{M_0}} M_T = \alpha\beta\gamma M_0(1-E_1) \frac{e^{-\frac{\alpha\tau}{T_2}} \sum_n^N B_1(n) e^{\frac{n\alpha\Delta t}{T_2}} \Delta t}{1-E_1\left[1-(\alpha\beta\gamma\Delta t)^2 \sum_n^N \sum_j^n B_1(n)B_1(j) e^{\frac{(j-n)\alpha\Delta t}{T_2}}\right]} \sim \frac{\alpha\beta e^{-\frac{\alpha\tau}{T_2}} f_0(\alpha)}{1-E_1+E_1(\alpha\beta\gamma\Delta t)^2 g_0(\alpha)} \qquad [2]$$

Where we have used the following definitions, which can be readily calculated form the RF profile, to simplify the equations:

$$f_0(\alpha) \equiv \sum_{n=1}^N B_1(n) e^{\frac{n\alpha\Delta t}{T_2}}, \quad f_1(\alpha) \equiv \sum_{n=1}^N nB_1(n) e^{\frac{n\alpha\Delta t}{T_2}}, \quad g_0(\alpha) \equiv \sum_{n=1}^N \sum_{j=1}^n B_1(n)B_1(j) e^{\frac{(j-n)\alpha\Delta t}{T_2}}, \quad g_1(\alpha) \equiv \sum_{n=1}^N \sum_{j=1}^n (j-n)B_1(n)B_1(j) e^{\frac{(j-n)\alpha\Delta t}{T_2}} \qquad [3]$$

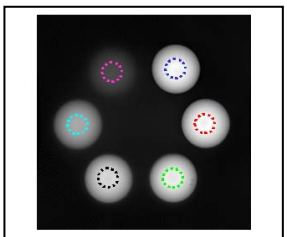
Fig.3:Experimental phantom setup

Maximizing MR signal:

In order to maximize the steady state transverse magnetization, one has two choices:

1) Keep τ fixed and optimize B_1, i.e. keep α fixed and optimize β.
2) Keep B_1 fixed and optimize τ, i.e. keep β fixed and optimize α.

Method 1) is mathematically simpler, and setting the derivative of Eq.[2] with respect to β to zero yields:

$$\beta = \frac{1}{\gamma\alpha\Delta t}\sqrt{\frac{1-E_1}{E_1 g_0}} = \frac{1}{\gamma\alpha\Delta t}\sqrt{\frac{1-E_1}{E_1\sum_{n=1}^N\sum_{j=1}^n B_1(n)B_1(j)e^{\frac{(j-n)\alpha\Delta t}{T_2}}}} \qquad [4]$$

One challenge with Eq.[4] is that the optimized RF amplitude βB_1 may be either higher than the hardware performance limit (and hence invalid) or significantly lower than the hardware performance limit, requiring iterative optimization to determine the best possible overall pulse.

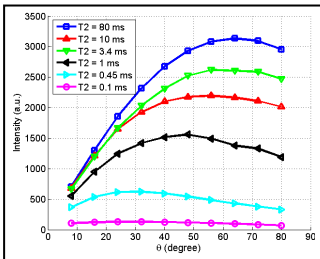

Fig.4a: Experimental signal intensities (const B_1)

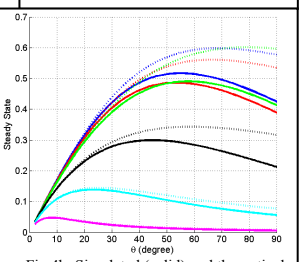

Fig.4b: Simulated (solid) and theoretical (dashed) signal intensities (const B_1)

Method 2) can be solved by setting the derivative of Eq.[2] with respect to α equal zero:

$$0 = \alpha^3\beta^2\gamma^2\Delta t_0^2 E_1 R_2\{\Delta t_0(f_1 g_0 - f_0 g_1) - \tau_0 f_0 g_0\} - \alpha^2\beta^2\gamma^2\Delta t_0^2 E_1 f_0 g_0 + \alpha R_2\{\tau_0 f_0(E_1-1) + \Delta t_0 f_1(1-E_1)\} + f_0(1-E_1) \qquad [5]$$

Once the optimum pulse parameters are determined, the optimum flip angle (generalized Ernst angle) can be calculated from the scaled RF profile. Fig.2 shows theoretical optimum flip angles (lines) vs. T_2 for several values of TR/T_1 along with simulated results (markers). Fig.2a shows the case for which the flip angle was varied by optimizing the RF amplitude (Eq.[4]) using a constant RF duration (τ = 0.5ms), while Fig2b shows the case for which the flip angle was varied by optimizing the RF duration (Eq.[5]) using a constant RF amplitude (B1 = 15μT). As was also observed in Ref.[6], the optimum flip angles for Fig.2a are always larger than the corresponding classical Ernst angles (horizontal lines), while the optimum flip angles for Fig.2b are always smaller (Ref.[2,3]). In both cases the optimum flip angles converge to the classical Ernst angle in the limit $T_2 \rightarrow \infty$.

Methods: Fig.3 shows the phantom setup consisting of spherical phantoms filled with water doped with Gadolinium and $MnCl_2$ resulting in measured T1 & T2 relaxation parameters shown in Table 1. UTE images were obtained at various flip angles using a constant RF amplitude and variable pulse durations of $\tau \approx$ 0.5ms – 5ms with TR = 50ms.

Results: The signal intensities measured in small ROIs at the center of each phantom are shown in Fig.4a as a function of nominal flip angles. The corresponding theoretical signal intensities using Eq.[2] (broken lines) and Bloch equation simulations (solid lines) are shown in Fig.4b. The classical and generalized Ernst angles (using Eq.[5]) as well as simulated and experimentally determined optimum flip angles are summarized in Table 1. Several features can be observed from Fig.4 and Table1: The simulated and experimental data agree well for all phantoms. The classical Ernst angle agrees with the simulated/experimentally optimum flip angles for longer T2 phantoms (columns 1-3), but breaks down for the three shortest T2 phantoms (columns 4-6) as expected. Finally, the generalized Ernst angle agrees well for the three shortest T2 phantoms but there are deviations for the longer T2 phantoms as a consequence of operating outside the low flip angle approximation. In vivo tissues generally have longer T1s than the phantoms used here, which means that the optimum flip angles are typically lower so that the small flip angle approximation is satisfied more readily.

	T1/T2 ≈ 90/80 [ms]	T1/T2 ≈ 85/10 [ms]	T1/T2 ≈ 49/3.4 [ms]	T1/T2 ≈ 20/1.0 [ms]	T1/T2 ≈ 15/0.45 [ms]	T1/T2 ≈ 10/0.1 [ms]
Classical Ernst	55°	56°	69°	85°	88°	90°
Generalized Ernst	69°	67°	79°	58°	25°	8°
Simulated Theta	55°	53°	58°	47°	23°	8°
Experimental Theta	62°	55°	65°	48°	27°	Too Low SNR

Table 1: Classical and generalized Ernst angles as well as simulated and experimental optimum flip angles for the phantom setup shown in Fig.3.

Conclusion: We have derived an analytic expression for the steady state transverse magnetization resulting from 2D UTE excitation RF pulses, which we used to predict the optimum flip angles (generalized Ernst angles) for short T2 tissues. Simulations and experimental verifications support the validity of the derived results.

References: [1] Tyler et al, JMRI 25:279 (2007) [2] Carl et al, MRM 64:481-490 (2010) [3] Carl et al, ISMRM (2009) [4] Robson et al, MRM 64:610-615 (2010) [5] Hargreaves et al, MRM 52:590–597 (2004) [6] Schick et al, JMR 206:88–96 (2010)